Some observations on the flow physics of paddle racquets

Francisco J Huera-Huarte

Proceedings of the Institution of Mechanical Engineers, Part P: Journal of Sports Engineering and Technology published online 10 September 2013
DOI: 10.1177/1754337113499324

Original Article

Institution of MECHANICAL ENGINEERS

Journal of SPORTS ENGINEERING AND TECHNOLOGY

Proc IMechE Part P:
J Sports Engineering and Technology
0(0) 1–9

DOI: 10.1177/1754337113499324
pip.sagepub.com
SAGE

Some observations on the flow physics of paddle racquets

Francisco J Huera-Huarte

Abstract

Paddle, padel or platform tennis is a rapidly growing sport derived from tennis, but played in smaller courts using a solid racquet, instead of a strung one. Most of the racquet manufacturers drill holes in the head arguing improved aerodynamic performances. The question is, if almost all manufacturers drill aerodynamic holes, are they optimally distributed from the fluid dynamics point of view? In this work, we use a generic racquet model to analyse what is the effect of the holes on the drag forces suffered by the racquet and how these forces are related to the wakes seen by the racquet during its motion. A porosity parameter is defined that takes into account not only the porosity itself but also how it is distributed within the racquet's head. Digital particle image velocimetry is used to quantify the flow field around the racquet, allowing the identification of different wake topologies that can be related to different drag performances.

Keywords

Paddle racquets, perforated disc wakes, aerodynamic holes, drag coefficients, digital particle image velocimetry

Date received: 25 April 2013; accepted: 3 July 2013

Introduction

Paddle, padel or platform tennis is a rapidly growing sport in terms of number of players, especially in the last decades. The racquets, like in all tennis-derived sports, consist of a handle and a head that in this case is not strung but solid. The aspect ratio of a general racquet, defined as the diameter of the head divided by its thickness, is about 6. Almost all paddle racquets have a common feature, what the manufacturers call aerodynamic holes. It appears evident that professional players prefer very rigid racquets and those that produce less damping during the impact of the ball.[1] Thus, drilling aerodynamic holes could negatively impact performance. The objective of this article is to study the drag forces on the racquet depending on porosity (ratio of hole area to racquet head area) and its distribution on the racquet head.

In general, most of the recent scientific investigations about racquets are related to tennis and racquet dynamic behaviour from a structural point of view.[2–5] Also, the interaction of the racquet with the human body has received attention in the past.[6–8] However, to the knowledge of the author, there are no scientific studies devoted to the understanding of the flow physics of paddle racquets. For fluid dynamic analysis purposes, a paddle racquet can be considered a perforated disc in cross-flow. The fluid dynamic forces acting on the head of the racquet are obviously largely affected by the wake the racquet generates when moved by the player, and hence, the performance of the racquet in the stages previous to the impact of the ball is mainly driven by the flow physics around the racquet. The manufacturers drill holes in the head arguing a better aerodynamic performance, but observing the existing commercial options, in terms of the number and distribution of holes, they seem to be randomly designed as there are no clear patterns. From a sports engineering perspective, the problem is unique of great complexity and does not appear to have been studied before.

The fluid dynamics of solid discs has been studied in the past.[9–11] If the plates or discs are perforated, the wake, the forces and the flow features change considerably. Relevant works with perforated, slotted or porous discs or plates in cross-flow have been published before.[12–15] In one of the most relevant works,[12] the author conducted wind tunnel experiments with

Department of Mechanical Engineering, Universitat Rovira i Virgili (URV), Tarragona, Spain

Corresponding author:
Francisco J Huera-Huarte, Department of Mechanical Engineering, Universitat Rovira i Virgili (URV), Av. Països Catalans, 26, 43007 Tarragona, Spain.
Email: francisco.huera@urv.cat

rectangular perforated plates and showed how for porosities under 20%, the drag practically does not vary, staying at values of about 1.4. The author related the drastic reduction of drag observed when porosities were higher than 20%, to the displacement of the vortex formation further downstream in the wake. This was associated with the air bleed resulting from the holes in the plate. In one of the previous works,[14] the authors observed the merge of the different jets formed in the holes of his experiment with a slotted plate, into stable structures that depending on how far away of the plate ended up being formed, resulted on reduced drag forces. The objective of this experiment is to quantify the forces and the wake behind the racquet, in order to relate the different wake structures to the forces exerted on the model, so a better understanding of the so-called aerodynamic holes can be achieved.

Experimental arrangements

A model of a generic racquet has been designed in acrylic material. The head of the racquet model consists of a disc with a diameter (D) of 130 mm and a thickness (e) of 19 mm, connected to a cylindrical handle made of the same material. This cylinder has an external diameter of 20 mm and a total length of 270 mm. The disc is perforated with 64 holes of radius (r) 3 mm separated in rows, by a centre-to-centre distance of 12 mm. Each hole in the racquet s head can be blocked easily yielding a solid and smooth surface, using modelling clay (plasticine), so different hole configurations can be imposed on the same model, and therefore, porosity changes are possible depending on the needs of the experiment. A standard racquet paddle appears in Figure 1.

Figure 1. A generic paddle racquet showing the so-called aerodynamic holes.

The experiments were conducted in the closed-loop recirculation free surface water channel (FSWC) at the Department of Mechanical Engineering of the Universitat Rovira i Virgili (URV) in Tarragona, Spain. The facility has a translucent working section made of glass, of dimensions $1 \times 1.1 \times 2.5$ m. With the water at its maximum height of 1 m, flow speeds of more than 0.7 m/s can be achieved with very low levels of turbulence intensity, in fact under 2.5%.

The main reason for conducting the experiments in water is the fact that a reduced scale model can be used, and this allows a larger Digital Particle Image Velocimetry (DPIV) field of view (FOV) in the wake of the racquet. Furthermore, the scaled model has a very small blockage ratio of less than 2% (surface normal to the flow upon the cross-sectional area of the water channel facility). The size of the model and the flow speeds generated in the water channel were also chosen in order to generate experiments with Reynolds numbers (Re) as near as possible to those in air, as in the real game situation. The Re is defined as the ratio of inertial forces to viscous forces ($\rho UD/\mu$), and in this case, it is based on the racquet head diameter D. ρ is the fluid density and μ is the dynamic viscosity of the fluid. In previous studies, Landlinger et al.[16] have shown how tennis racquets can travel as fast as 30 m/s at the moment of impact with the ball, when used by elite or professional players. Although it seems that there are no similar studies showing padel racquet speeds, it is believed that this velocity is considerably smaller. Still, if speeds as high as 10 m/s are considered, Re can end up being over 180,000. In these experiments, Re of more than 60,000 was reached in order to be as close as possible to the real game situation in the lab. At these very high Re, the main features in the wake of the disc are believed to be very similar. In fact, in a previous study with slotted discs in cross-flow,[14] the authors conducted experiments at Re up to 18,000 and concluded that practically no differences arose in the wake if Re were over 7400.

On the other hand, fluid–structure interaction phenomena have been neglected as it is thought not to be important in the aerodynamics of racquets. The fluid dynamic periodic and time-varying forces induced by the wake are small and do not affect the motion imposed by the player. Therefore, for the experiments, a very high rigidity was imposed to the model with the objective of keeping the bluff body completely stationary during all the tests carried out.

In order to measure the forces on the racquet model, a strain gauge–based six-axis force balance was used. The load cell system was attached to a fixed structure hanging on top of the working section, and the racquet model was connected to the sensor, ensuring that all forces and moments experienced by the model were transferred to the balance. A Cartesian reference system with its centre coincident with the centre of the disc is defined, having the positive part of the x-axis perpendicular to the disc in the direction of the flow in the

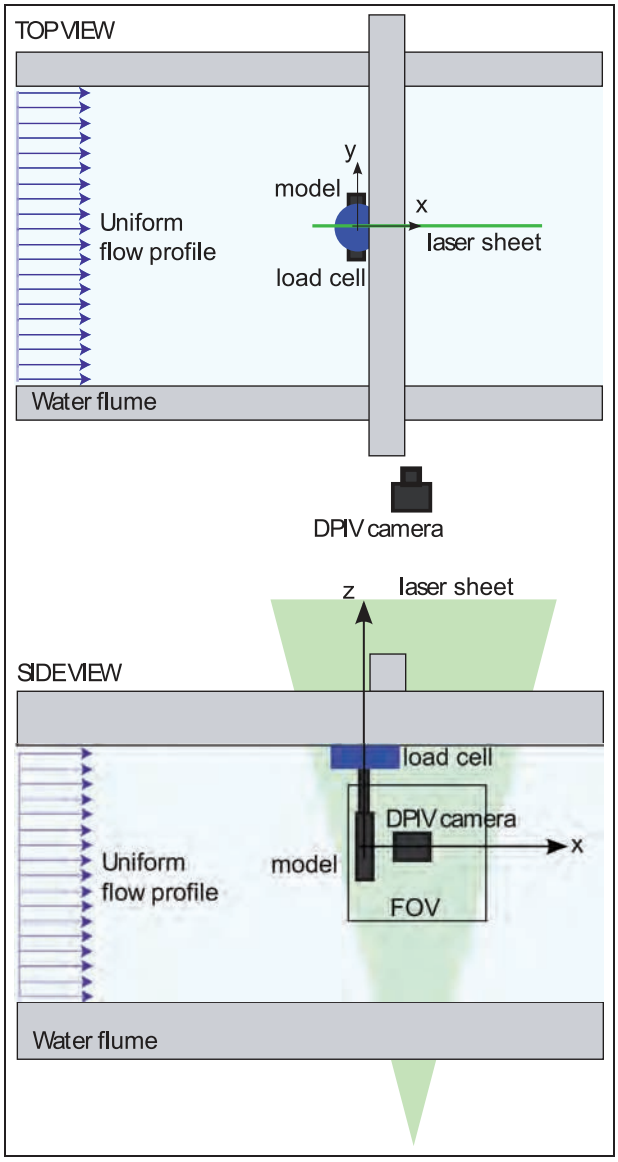

Figure 2. Set-up of the experiment.
DPIV: digital particle image velocimetry; FOV: field of view.
The racquet model appears in black connected to the balance, which is depicted in blue.

channel, y is perpendicular to the flow direction and z coincides with the axis of the handle, see Figure 2, for details. The balance has a resolution of 0.025 N in F_x and F_y, of 0.05N in F_z and of 0.031 N m for the three moments M_x, M_y and M_z.

The wake of the racquet model was investigated using DPIV. In DPIV,[17] the flow is seeded with particles of several microns and the flow is illuminated by a planar pulsed laser sheet. The particles scatter the light and a high-speed camera, synchronised with the laser pulses, records the images of the illuminated particles. Image processing of the obtained images allows the calculation of the velocity flow field.

For this set-up, a camera based on a 12-bit charge-coupled device (CCD) sensor with a pixel size of 7.4 × 7.4 μm and a resolution of 4 MPixel (2048 × 2048) was used to capture the images of the illuminated seeded flow. A 50 mm fixed focal length lens was used in combination with the described camera, in order to capture images covering a FOV in the xz plane, of more than three disc diameters downstream the model in the x direction, and three diameters in the z direction, distributed symmetrically about the centre of the model. Each one of the heads of the Nd:YAG 532 nm green laser used for the experiments was able to produce up to 200 mJ pulses at a rate of 15 Hz. By triggering each laser beam at 15 Hz with a very small delay (Δt) between them, the FOV was illuminated twice every 1/15th of a second. The synchronisation of the laser with the camera by means of the same trigger signal allowed the acquisition of a pair of images of the illuminated particles in the FOV, every 1/15th of a second. A Δt of 3.5 ms was used for the experiments. After the image processing, which involved several steps, velocity fields in the wake of the racquet model were obtained every 1/15th of a second.

Briefly, the image processing consisted of an initial step in which regions of the image that do not include seeding particles, such as the racquet itself, were masked. A cross-correlation algorithm[17] was applied to the masked images, based on an interrogation area of 32 × 32 pixels with 50% of area overlapping. Outlier vectors output by the cross-correlation scheme were identified after comparison with neighbouring vectors and replaced by new values obtained from averaging around the outlier. Quantities derived from the flow field such as vorticity, that will be presented later on in section Results and discussion , together with the flow fields, required a last step involving a moving average filter with the objective of removing background noise, which can be especially problematic when calculating derivatives. Figure 2 depicts in detail the layout of the experiment together with the DPIV system set-up in the FSWC.

Results and discussion

A total of six different racquet head configurations were considered, namely racquet models R0, R1, R2, R3, R4 and R5, as depicted in Figure 3. Each one had a different porosity and a different porosity distribution, resulting from different hole patterns.

Table 1 gives the details associated with each racquet configuration. The second column in this table is the number of holes in each model (n), the third column is the dimensionless mean radius of porosity (δ), the fourth column is the ratio of hole area to racquet head area (β) and the last column is the porosity parameter (γ).

The dimensionless mean radius of porosity δ results from dividing the mean radius of porosity (d_m) by the diameter of the racquet s head (D). The holes in each configuration are distributed radially around the axis of the racquet s head. This radial distribution of holes can

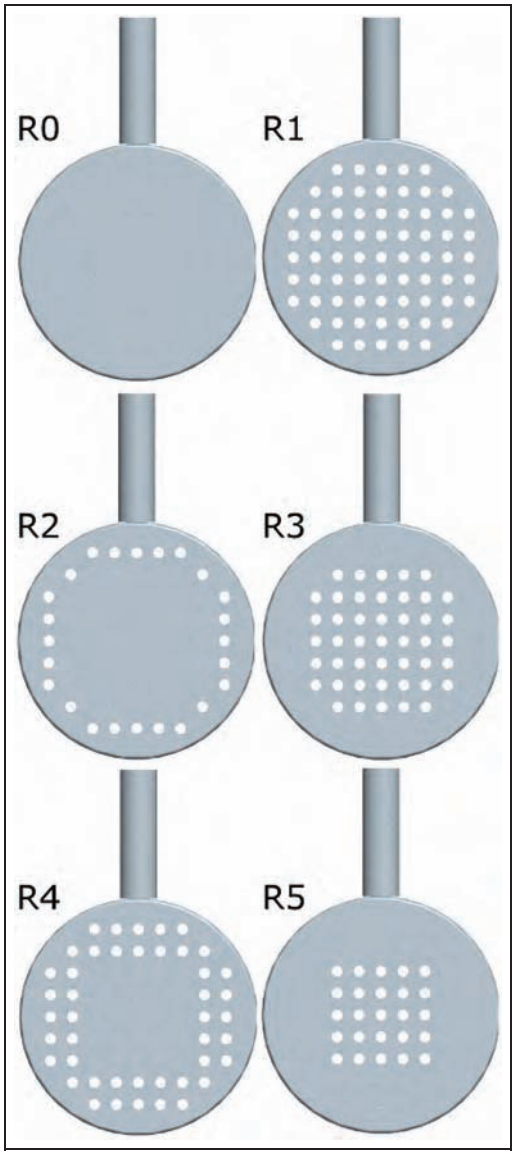

Figure 3. Different hole configurations in the racquet's head used for the experiments.

Table 1. Experiment parameters.

Case	n	δ	β	γ
R0	0	1	0	1
R1	69	0.49	14.7	0.72
R2	24	0.85	5.1	0.71
R3	45	0.39	9.6	0.88
R4	44	0.69	9.4	0.64
R5	25	0.29	5.3	0.96

be seen in Figure 4, where a total of four radii appear indicated, one for each row of holes in the racquet head. d_m is the mean of all the rings participating in each configuration presented in Figure 3. For example, d_m, in configuration R4, is the mean diameter resulting from the two outer circles, that is twice $(50.5 + 39.1)/2$. The area parameter (β) is defined as the area of holes,

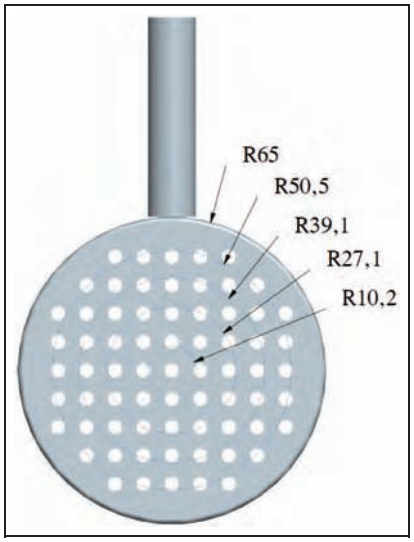

Figure 4. Detail of the racquet model with the hole radii depicted.

divided by the total area of the disc, $\beta = 4nr^2/D^2$. The parameter γ is defined with the objective to take into account how the holes are distributed in the racquet s head. It is calculated as in equation (1) and is the result of computing the area polar inertia of each racquet s head configuration, divided by the inertia of the solid racquet s head area

$$\gamma = 1 - \frac{32nr^2}{D^4}\left(\frac{r^2}{2} + d_m^2\right) \tag{1}$$

Drag coefficients (C_d) were calculated after measuring the forces in experiments of more than 30 s, as the ratio between the mean force registered during the experiment and the dynamic pressure times the cross-sectional area of the model (A), as in equation (2)

$$Cd = \frac{F_x}{\frac{1}{2}\rho U^2 A} \tag{2}$$

The drag coefficients on the racquet appear in Figure 5, plotted against γ, so the influence of the porosity and its distribution on the model head can be observed. The first thing to note is that the differences in the force coefficients between all the cases studied are small, as expected from the results of other researchers with perforated plates.[12] This author showed how the drag coefficient decreased very slowly by increasing evenly distributed porosity in his experiment, when β was smaller than 20%. On the other hand, he also showed how small increases of porosity for values of β larger than 20% resulted in large drag reductions. Paddle racquets are characterised by very low porosity values in the order of $10\% < \beta < 20\%$, so in the present experiments with $\beta < 15\%$, the drag coefficient should not be largely modified by making the porosity of the paddle smaller. Moreover, keeping porosity low seems to be a must for the racquet performance,[1] so it is

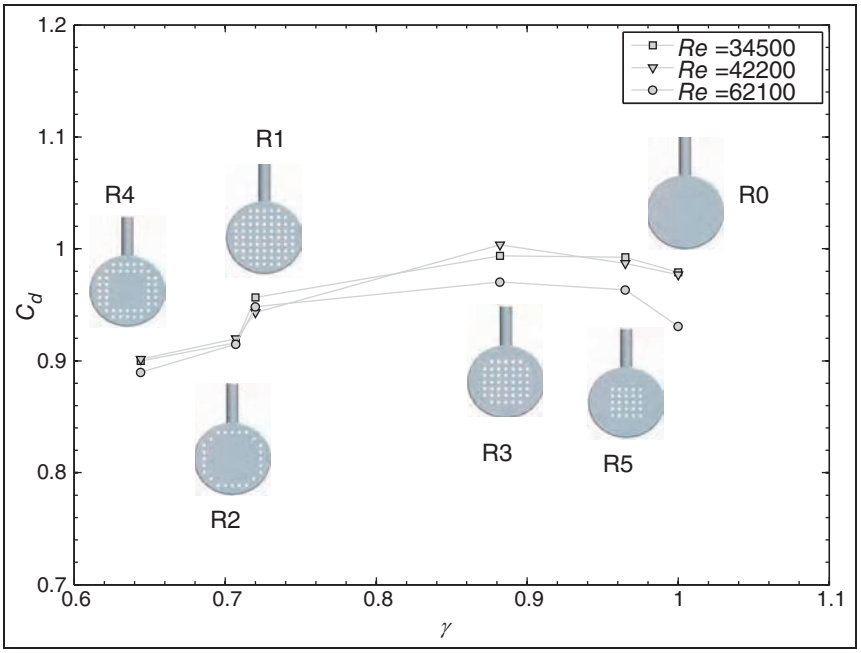

Figure 5. Drag coefficients as a function of γ.

necessary to better understand what is the role of the different hole patterns.

The drag coefficients (C_d) are presented for three Reynolds numbers (Re), in the range that goes from 34,500 to 62,100. The coefficients are slightly smaller at higher Re, if low γ are configured in the racquet, and they all show the same trend: The configurations showing low drag are not those with a larger number of holes and therefore larger β, but those with the lowest γ. This means that there is a clear relationship between the location of the holes and drag, and therefore, it is not only a question of porosity. The best two configurations are racquet models R2 and R4 (see Figure 3), which are the models with the holes distributed in the outer part of the racquet head. Model R3 is the closest to the generic commercially available racquet, and it is curiously the one that produces the largest drag. It is true that in terms of forces experienced by the player, any solution will end up in very low drag forces, but still overall drag reductions up to a 10% can be achieved by simply distributing the holes at a certain distance from the head s centre, as in models R2 and R4, and even though in this study structural implications were not investigated, it is clear that leaving the centre of the head empty of holes, where most of the ball impacts are received, should be better for racquet rigidity and fatigue issues. As Figure 5 shows, the lowest drag configurations are also those that should produce the best structural performance[1] and fatigue resistance.

The relationship between the force coefficients from Figure 5 and the wake generated by the racquet in each configuration can be inferred from the DPIV data. The objective was to find out what were the main features for some of the most interesting hole patterns studied. DPIV results are presented in Figures 6–8 for the cases with the intermediate Re. The first figure is for case R0, the solid racquet without holes in the head and a $\gamma = 0$. In plot 6(a), the dimensionless mean flow velocity in the x direction or $u(x, z)/U$ is shown by means of a colour map. Streamlines are also shown for clarity. The mean flow field was measured in a plane perpendicular to the racquet s head that contains the axis of the handle and the centre point of the racquet head, that is at a $y/D = 0$. Red indicates velocities with values close to the free stream, while blue is used for reversed flow regions. The grey area in the plot is the mask applied to the DPIV images for processing the results and indicates the location of the racquet model. Both axes x and z are normalised with the head diameter D. As already explained in section Experimental arrangements , the Cartesian coordinate origin is located at the centre of the model. Plot 6(b) is for the mean dimensionless vorticity field $\omega(x, z)D/U$. In this case, the wake extends several diameters downstream of the model showing a large recirculation region of more than two head diameters behind the model. The lower shear layer has larger values of vorticity as the upper one is largely affected by the racquet s handle because the DPIV plane is at $y/D = 0$. These large values of vorticity near the shear layers extend to more than 1 diameter downstream the model. Two main eddy structures can be inferred from the mean fields at a distance of about 0.8 diameters downstream the model. The eddies seen in the mean flow indicate the position at which the shear layers roll up intermittently, as is characteristic in the flow around discs.[12,14,18]

If a region of porosity is introduced at the centre of the racquet head, as in configurations R1, R3 and R5 with $\gamma = 0.72$, 0.88 and 0.96, respectively, a bleed zone is formed resulting from the equally spaced jets. The

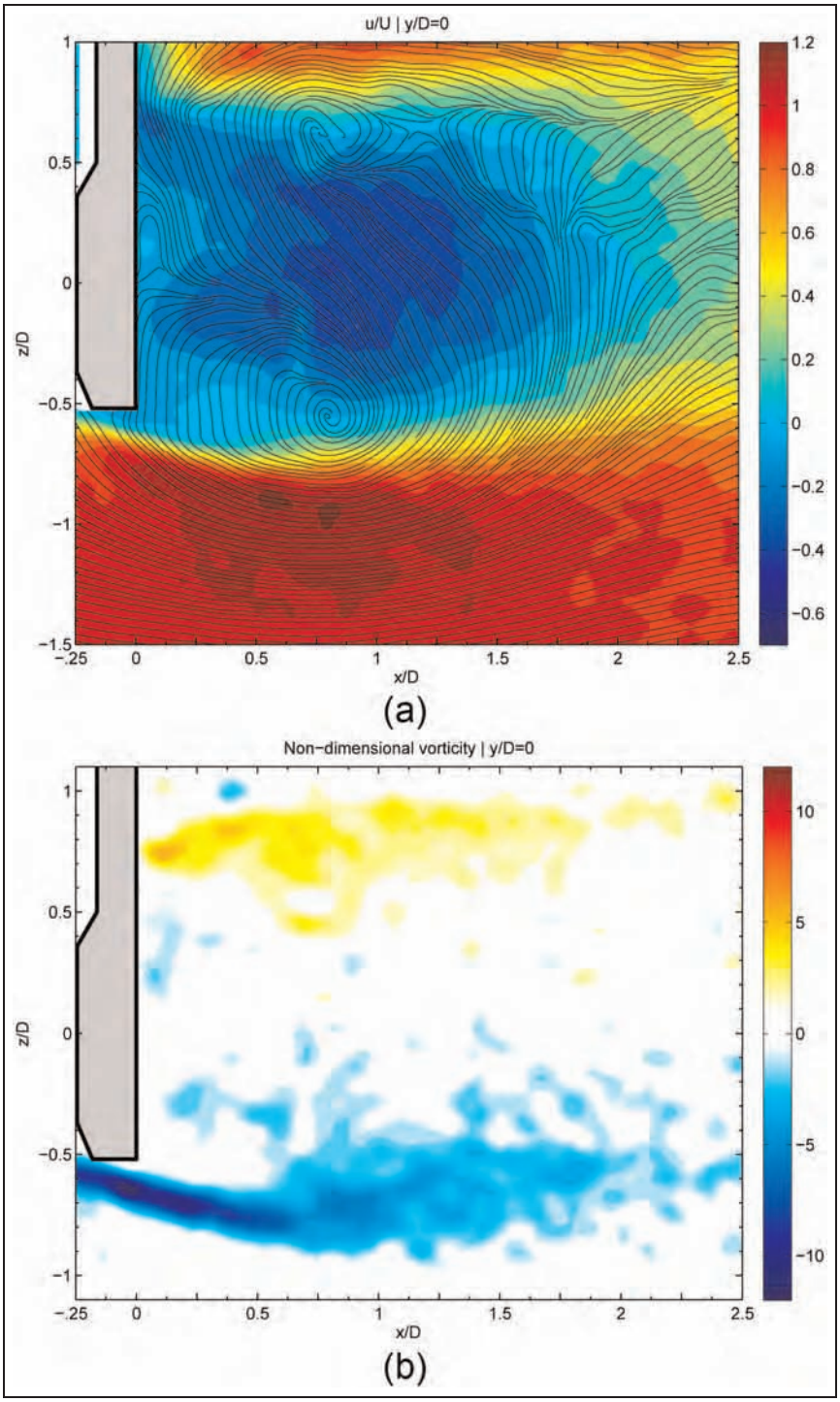

Figure 6. DPIV results for configuration R0 in the plane y/D=0: (a) *u/U* and streamlines and (b) non-dimensional vorticity field.

bleed region largely modifies the near wake region. The extreme case for this type of bleed would be configuration R1, for which the largest porosity was set. In Figure 7(a), the central region of the near wake is characterised by positive velocities and the reversed flow region has smaller velocities when compared to those seen in Figure 6(a). The two main eddies are now further downstream, at about 1.2 diameters from the model, when compared to the case R0. Moreover, the bleed produces a secondary structure in the very near wake of the model s head that can be seen either in the streamlines or in the vorticity plot. The vorticity resulting from the central region jets interacts with the vorticity in the shear layers and makes them weaker as they are opposite sign. The jets in the central region of the racquet move far away from the model the recirculation bubble generated in the wake. In the case with no porosity (R0), the reversed flow bubble starts immediately downstream the model, extending from $x/D = 0$ to a stagnation point at about $x/D = 2$. In

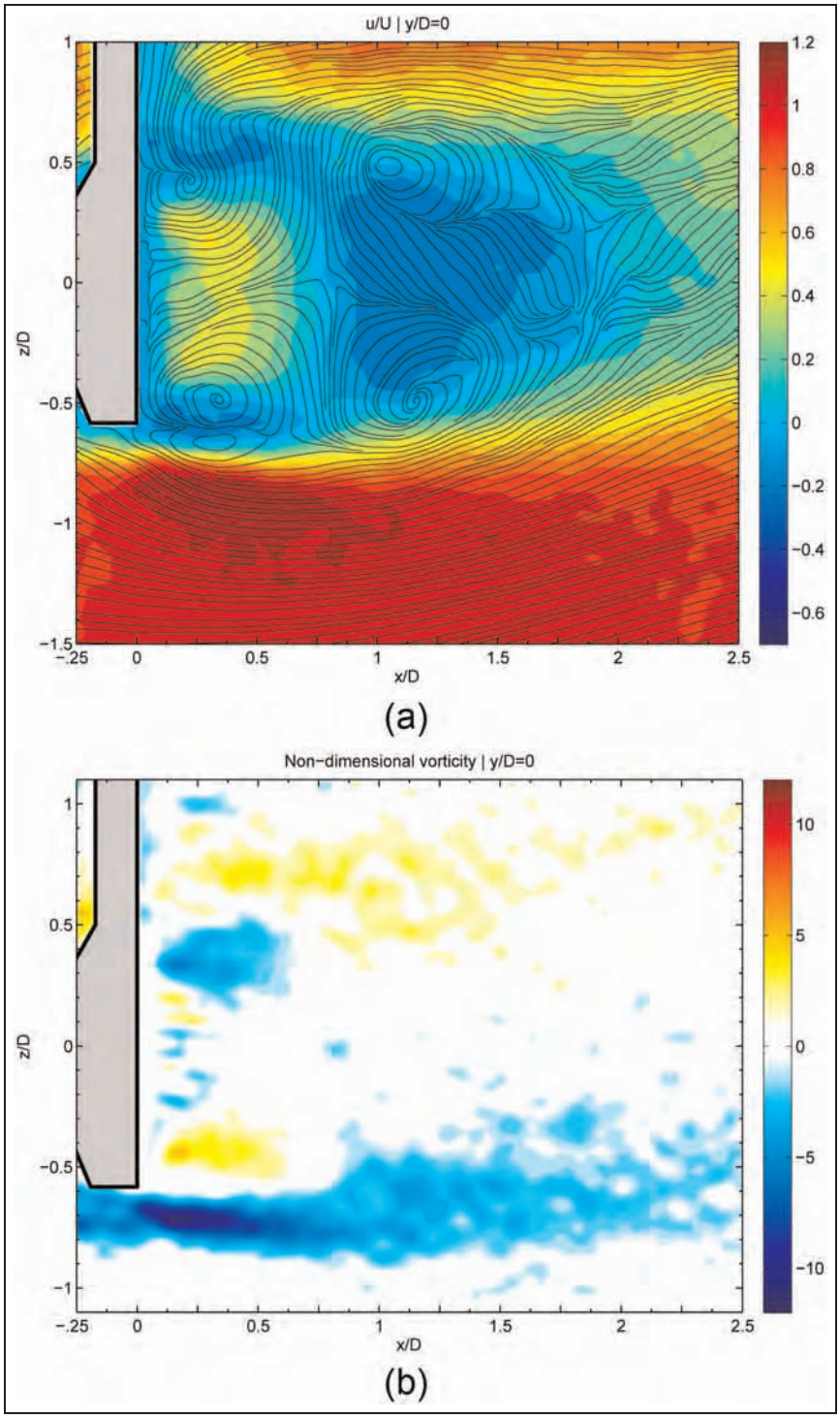

Figure 7. DPIV results for configuration R1 in the plane y/D=0: (a) *u*/*U* and streamlines and (b) non-dimensional vorticity field.

configuration R1, the bubble becomes considerably smaller and it stays confined between a first stagnation point at an $x/D = 0.75$ and a second one further downstream at $x/D = 1.75$.

In the other configurations, the bleed is introduced through an annular region of porosity near the racquet s head edges, such as in configurations R2 and R4 with $\gamma =$ of 0.71 and 0.64, respectively. Even though in these two cases β is similar or smaller than in cases R1, R3 and R5, Figure 5 shows smaller drag coefficients. This can be explained by observing the DPIV results in Figure 8 from case R2. The interaction between the bleed vorticity and the vorticity in the shear layers is even stronger, and even though the size of the recirculation bubble is not affected in the x direction, it becomes significantly reduced in the z direction.

The effect of the porosity is clear[12] in rectangular perforated plates with high porosity: Porosity reduces

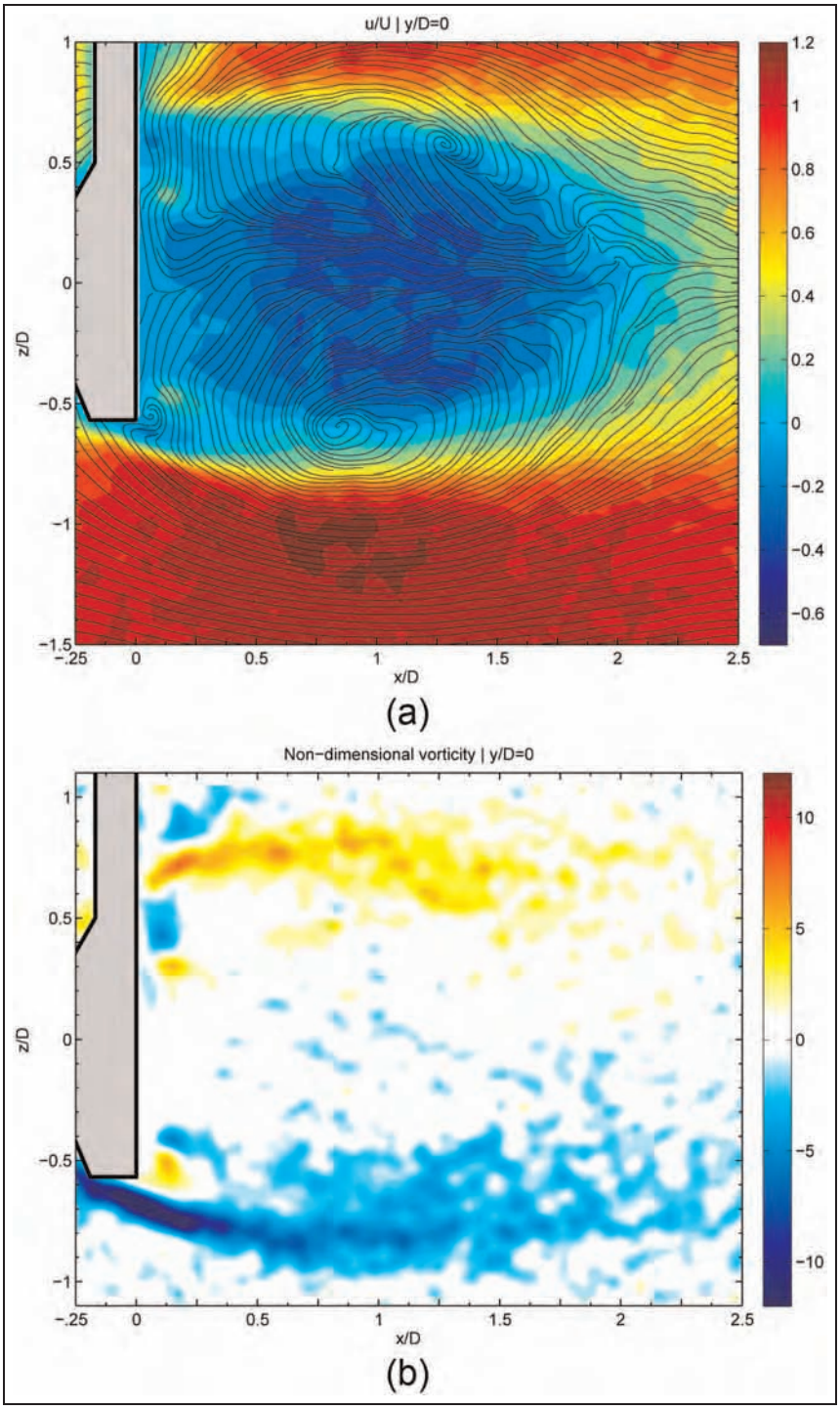

Figure 8. DPIV results for configuration R2 in the plane y/D=0: (a) *u/U* and streamlines and (b) non-dimensional vorticity field.

the drag by moving the recirculation region in the wake, to points further away from the bluff body, so the shear layer interacts at larger distance from it. This is confirmed now, thanks to these quantitative DPIV measurements, even if porosities are very low.

Conclusion

Experiments with a perforated disc in cross-flow have been made in order to study the flow physics of paddle racquets. The forces and the wake of the racquet were quantified using a multi-axis load cell and DPIV, respectively. Several previous studies were carried out with perforated or slotted plates and discs, but to the knowledge of the author, none of them were directly applied to the rigorous study of the fluid dynamics of rigid perforated sports racquets.

At the low values of porosity seen in paddle racquets, a parameter that only accounts for the ratio of open area to solid area of the racquet is not enough to

describe the physics. A parameter γ that accounts not only for the porosity (i.e. the number of holes and its size) but also for its distribution on the racquet head was used for this study.

It seems that the actual design of the racquets, in terms of their so-called aerodynamic holes, has not received scientific attention until now, as there is no evidence of works investigating how the holes should be distributed on the racquet s head. The first important observation is that for the very low porosities in racquets available in the market, very small differences exist in terms of drag. The smaller drag coefficients were found to be produced by a large diameter annular distribution of holes near the edges of the racquet s head. When the holes are arranged at the outer parts of the racquet head, a strong interaction with the separated shear layers detaching from the racquet head edge is produced, yielding smaller drag coefficients. Even though in this work structural investigations were not carried out, it appears to be evident that leaving the central region of the head free of holes contributes to have a more rigid racquet with less damping, which seems to be good for performance, as previous authors have suggested.[1] Also, the hole configuration proposed here can lead to longer lasting racquets.

Acknowledgement

The author would like to thank the model manufacturing work done by Mr Vicens Puig.

Declaration of conflicting interests

The authors declare that there is no conflict of interest.

Funding

This study was funded by the Plan Nacional I + D + I of the Spanish Ministerio de Ciencia e Innovación (grant DPI2009-07104).

References

1. Overney LS, Michaud V, Fischer C, et al. Carbon outclasses wood in racket paddles: ratings of expert and intermediate tennis players. *J Sport Sci* 2010; 28(13): 1451–1458.
2. Allen T, Hart J, Spurr J, et al. Validated dynamic analysis of real sports equipment using finite element; a case study using tennis rackets. *Procedia Eng* 2010; 2(2): 3275–3280.
3. Banwell G, Mohr S, Rothberg S, et al. Using experimental modal analysis to validate a finite element model of a tennis racket. *Procedia Eng* 2012; 34: 688–693.
4. Mucchi E. On the sweet spot estimation in beach tennis rackets. *Measurement* 2013; 46: 1399–1410.
5. Valentine RM. Application of sensors to investigate tennis racquet dynamics. *Procedia Eng* 2012; 34: 449–454.
6. Bower R and Cross R. Player sensitivity to changes in string tension in a tennis racket. *J Sci Med Sport* 2003; 6: 120–131.
7. Hennig EM, Milani TL and Rosenbaum D. The influence of tennis racket design on impact induced arm oscillations. *J Biomech* 1994; 27(6): 669.
8. King MA, Kentel BB and Mitchell SR. The effects of ball impact location and grip tightness on the arm, racquet and ball for one-handed tennis backhand groundstrokes. *J Biomech* 2012; 45: 1048–1052.
9. Bearman PW. An investigation of the forces on flat plates normal to a turbulent flow. *J Fluid Mech* 1971; 46(1): 177–198.
10. Lee SJ and Bearman PW. An experimental investigation of the wake structure behind a disk. *J Fluid Struct* 1992; 6: 437–450.
11. Miau JJ, Leu TS, Liu TW, et al. On vortex shedding behind a circular disk. *Exp Fluids* 1997; 23: 225–233.
12. Castro IP. Wake characteristics of two-dimensional perforated plates normal to an air-stream. *J Fluid Mech* 1971; 46(3): 599–609.
13. Higuchi H. Experimental investigation of the flowfield behind grid models. *J Aircraft* 1989; 26(4): 308–314.
14. Higuchi H, Zhang J, Furuya S, et al. Immediate and near wake flow patterns of slotted disks. *AIAA J* 1998; 36(9): 1626–1634.
15. Villermaux E and Hopfinger EJ. Periodically arranged co-flowing jets. *J Fluid Mech* 1994; 263: 63–92.
16. Landlinger J, Lindinger S, Stöggl T, et al. Key factors and timing patterns in the tennis forehand of different skill levels. *J Sport Sci Med* 2010; 9: 643–651.
17. Willert C and Gharib M. Digital particle image velocimetry. *Exp Fluids* 1991; 10: 181–193.
18. Marshall D and Stanton TE. On the eddy system in the wake of flat circular plates in three dimensional flow. *P Roy Soc A: Math Phy* 1931; 130(813): 295–301.